

Fluid inclusions in celestine and their significance in the study of the formation of the native sulphur deposits in the Carpathian Foredeep

JAN PARAFINIUK¹, ARKADIUSZ GAŚIŃSKI² and ANDRZEJ KOZŁOWSKI¹

¹ Department of Geology, University of Warsaw, Żwirki i Wigury 93, 02-089 Warsaw, Poland; e-mails: j.parafiniuk@uw.edu.pl; a.j.kozlowski@uw.edu.pl

² Institute of Ceramics and Building Materials, Postępu 9, 02-676 Warsaw, Poland; e-mail: arkadiusz.gasinski@icimb.lukasiewicz.gov.pl

ABSTRACT:

Parafiniuk, J., Gaśniński, A. and Kozłowski, A. 2025. Fluid inclusions in celestine and their significance in the study of the formation of the native sulphur deposits in the Carpathian Foredeep. *Acta Geologica Polonica*, **75** (2), e42.

Celestine is a rather common mineral in epigenetic native sulphur deposits and seems to be a very valuable indicator of some of the geological processes forming these deposits. This paper presents the results of investigation of fluid inclusions in celestine from the Tarnobrzeg native sulphur deposits (SE Poland). Several different morphological types of celestine were selected from Machów open-pit mine. Study of the fluid inclusions has been carried out using microscopic and microthermometric methods. The data show that two types of chloride fluids were responsible for the formation of celestine and native sulphur and further transformation of the native sulphur deposits. The first type of fluid, containing a relatively higher salt content and lower NaCl/CaCl₂ ratio, also points to the role of hydrocarbons during the formation of native sulphur deposits. The second type of fluid contains a relatively lower amount of salt and a higher NaCl/CaCl₂ proportion and reflects the subsequent evolution of the chemistry of the fluids forming the deposits. The results of the study of fluid inclusions in celestine are in good agreement with its stable isotope composition.

Key words: Carpathian Foredeep; Celestine; Fluid inclusions; Epigenetic native sulphur deposits.

INTRODUCTION

Despite more than 50 years of geological, hydrogeological and mineralogical investigations many aspects of the formation of Carpathian Foredeep sulphur deposits are not fully understood. Most geologists claim the epigenetic formation of these deposits (e.g., Pawłowski *et al.* 1985). However, some authors suggest their syngenetic origin (Gaśiewicz 2000a). Many papers considering the role of microorganisms (Krouse and McCreedy 1979; Pawlikowski 2023), hydrocarbons (Pawłowski *et al.* 1985; Parafiniuk *et al.* 1994), and karst (Osmólski 1976; Klimchouk

1997) in the genesis of native sulphur have been published. The results of mineralogical, geochemical and stable isotope studies were presented by Parafiniuk (1989a), Peryt *et al.* (2002), Böttcher and Parafiniuk (1998), Gaśiewicz (2000b), Bąbel (2004), and Kasprzyk *et al.* (2007). In addition, some fluid inclusion studies on minerals (gypsum and native sulphur) from native sulphur deposits of the Carpathian Foredeep have been carried out (Poberegsky 1993, Petrichenko *et al.* 1997). But no data concerning fluid inclusions in celestine from the sulphur deposits of the Tarnobrzeg area exist. Celestine seems to be very important mineral pointing out many aspects



of the conditions under which the deposits formed (Parafiniuk and Hałas 1997).

Fluid inclusions studies can provide very useful information about the conditions during different stages of rock evolution (Van den Kerkhof and Hein 2001; Goldstein 2001). Also fluid inclusions in celestine have been the object of earlier investigation (Parnell *et al.* 2000). Fortunately, most of the celestine crystals of the Tarnobrzeg area contain fluid inclusions that can be observed and investigated. The main aim of this study was to research the composition of fluid inclusions in celestine from the Tarnobrzeg native sulphur deposit and to see if it will bring new light in explaining the condition of formation of the deposit.

GEOLOGICAL SETTING

The Early to Middle-Miocene Carpathian Foredeep Basin developed on the southern edge of the European Platform at the front of the overriding Carpathian accretionary wedge (Text-fig. 1). The outer sub-basin of the foredeep is filled with Middle-Miocene marine deposits up to 3500 m thick. The Carpathian Foredeep basin was affected by two salinity crises. During the Late Badenian main event gypsum was deposited throughout most of the foredeep basin, whereas in the most internal isolated areas halite and sporadically potash evaporites were precipitated (Ślącza and Oszczytko 2002). The Middle-Miocene gypsum and anhydrite beds in the Carpathian Foredeep contain many native sulphur deposits of economic importance. In the Polish part of the foredeep these deposits mostly consist of sulphur-bearing limestones embedded in gypsum layers (Nieć and Sermet, 2013).

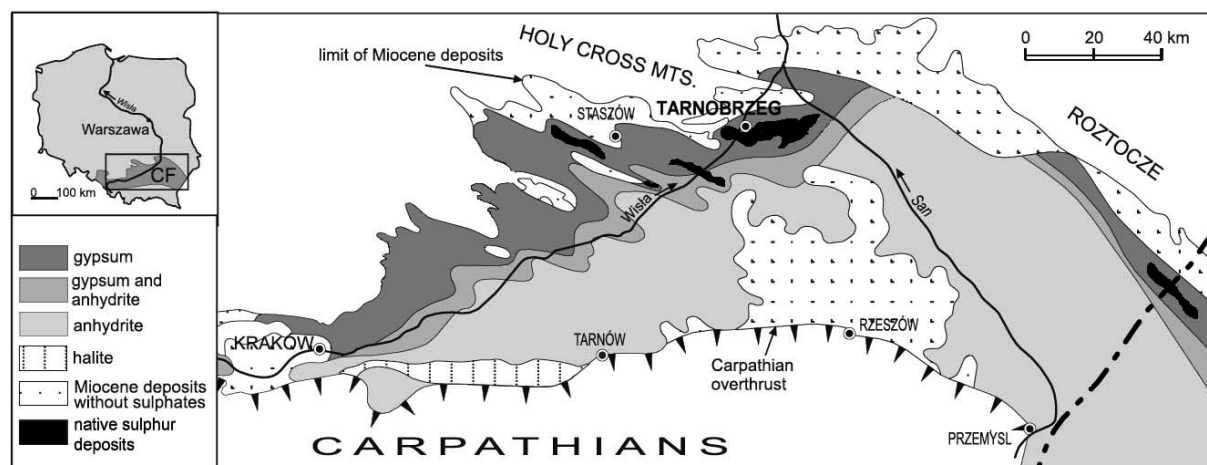
The large native sulphur deposits are located in the Tarnobrzeg area and were previously intensively exploited by open-pit and underground melting methods. The Machów mine was one of the biggest open-cast sulphur mines in Europe. Mining activity there created a unique opportunity to collect and to investigate mineralogical samples before the mine was closed down in 1992. Recently the Machów mine has been filled with water to form a reservoir used for recreation.

MINERALOGY OF CELESTINE OF THE TARNOBRZEG AREA

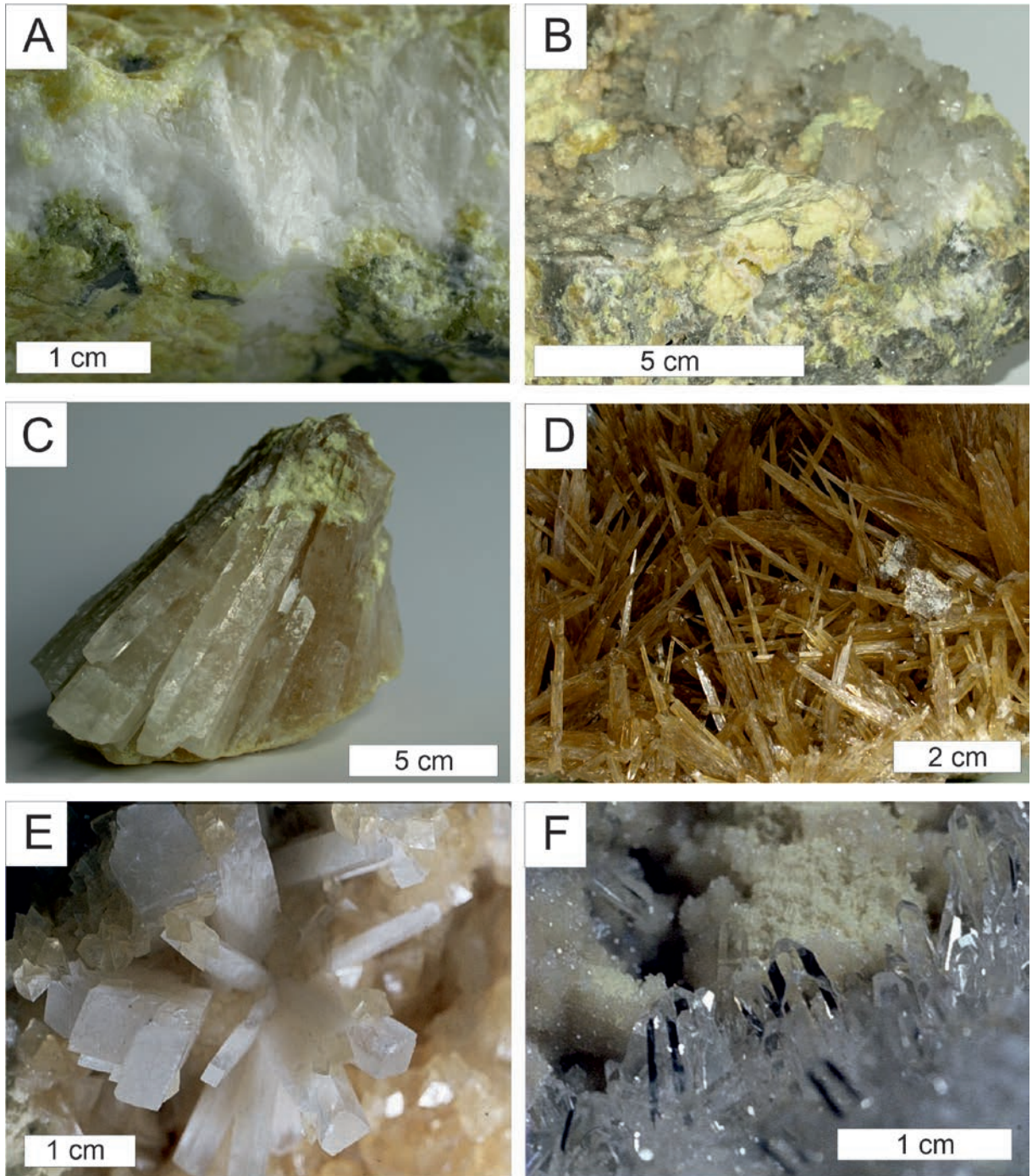
The main constituents of the Machów deposit are calcite and native sulphur. The accessory minerals include celestine, barite, gypsum, subordinately strontianite and aragonite (Kowalski *et al.* 1980; Pilichowska 1984; Parafiniuk 1989a, 2023). Celestine (SrSO_4) is a mineral often occurring in gypsiferous rocks and post-gypsum sulphur-bearing limestones. Several morphological types of celestine from Machów mine have been described previously (Parafiniuk 1989a):

- white, radial or parallel aggregates of fibrous celestine filling veins, cavities and geodes in limestone;
- fan-shape yellow to dark brown aggregates of acicular crystals;
- prismatic, often water-clear crystals; this type of celestine often contains inclusions of native sulphur;
- wedge-shaped flat terminated aggregates of pale-blue celestine changing in the lower part into whitish intergrowths of celestine with older strontianite

Representative examples of the morphological varieties of celestine are shown in Text-fig. 2. Every



Text-fig. 1. Distribution of Badenian evaporates in the Carpathian Foredeep in Poland (after Kasprzyk *et al.* 2007).

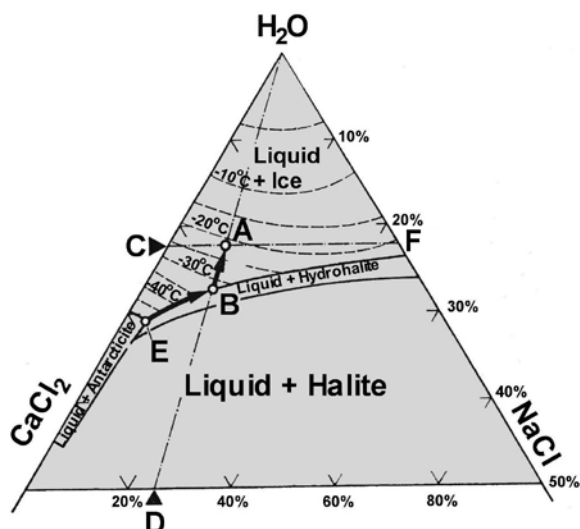


Text-fig. 2. Morphological variety of celestine from the Machów mine. A – Compact celestine aggregates forming veinlet in the sulphur-bearing limestone, B – short-prismatic celestine crystals covering fragments of the sulphur-bearing limestone, C – radial aggregate of prismatic crystals with inclusion of native sulphur, D – sprays of acicular brown crystals, E – pale-blue stubby celestine with strontianite intergrowths in the basal parts, F – druse of transparent, well developed crystals.

variety contains fluid inclusions which could be examined in this study. These inclusions can be a very valuable indicator of the environmental conditions during the formation of sulphur-bearing rocks.

METHODS

From each morphological type of celestine two to four samples were selected. The specimens were



Text-fig. 3. A phase diagram for the system NaCl-CaCl₂-H₂O illustrating the method for estimating the composition of an initially frozen fluid inclusion (after Kozłowski 1984; Williams-Jones and Samson 1990).

prepared in the form of thin mineral plates (about 200–500 mm in thickness) polished on both sides. The plates were glued by epoxy resin onto a glass slide. Firstly, the specimens were examined using optical microscopy in the transmission light mode and in the reflection UV mode at room temperature.

The next step was to investigate the fluid inclusions containing water solution. Such research is carried out using routine homogenization and freezing methods (Roedder 1984); the dual-purpose heating-freezing microscope stage (type Fluid Co) was used. The first step was microthermometric cooling of fluid inclusions. After such inclusions had been frozen the eutectic melting temperatures were observed. This temperature gave information about which general model can be best applied to these inclusions. The next thing was the determination of the ion ratio and salinity using microthermometric observations of intermediate melting events and a final melting event.

The studied inclusions typically yielded an eutectic melting temperature of a little below -50°C . This temperature suggests the applicability of the H₂O-NaCl-CaCl₂ system. The equilibrium eutectic for this system is at -52°C , so a defined eutectic melting at this temperature is a positive indication that this system applies. Aqueous solutions dominated by NaCl and CaCl₂ are well known from sedimentary basins where brines have undergone significant rock-water interactions. Text-fig. 3 shows the phase diagram for this system.

Microthermometric observations during heating of previously frozen inclusions has shown the melting down of antarcticite (CaCl₂·6H₂O) at a temperature of approximately -52°C (point E on Text-fig. 3). Further heating changed the composition of the liquid along the cotectic curve, until the last portion of hydrohalite (NaCl·2H₂O) was melted down (point B). This point was used to estimate the CaCl₂/NaCl ratio. The straight line connecting point B and the H₂O peak of the ternary diagram crosses the CaCl₂-NaCl baseline at point D. This point denoted the ratio of CaCl₂ and NaCl (in weight percent). The last phase melting down during the continuous heating of the preparate was ice. The straight line parallel to the CaCl₂-NaCl baseline drawn through point A (the final meltdown of ice) indicates the approximate total salinity of the trapped inclusion (point F, wt % equivalent NaCl).

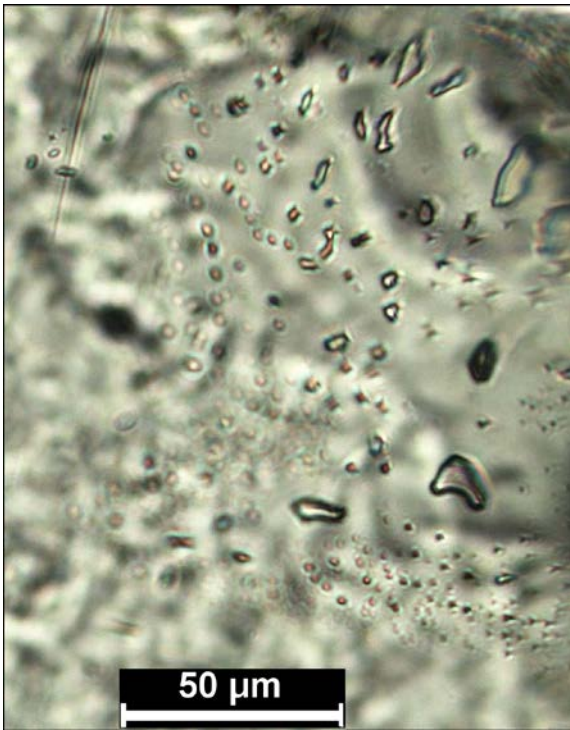
The last thing was to open some inclusions containing the vapor phase and to extract this phase using a microsyringe. Then the vapor phase reacted with suitable chemicals and the volume of the bubble gave some information about gas proportions in the initial composition. The rest of the bubble neutral to the reagent was assumed to be N₂.

DESCRIPTION OF FLUID INCLUSIONS IN CELESTINE CRYSTALS

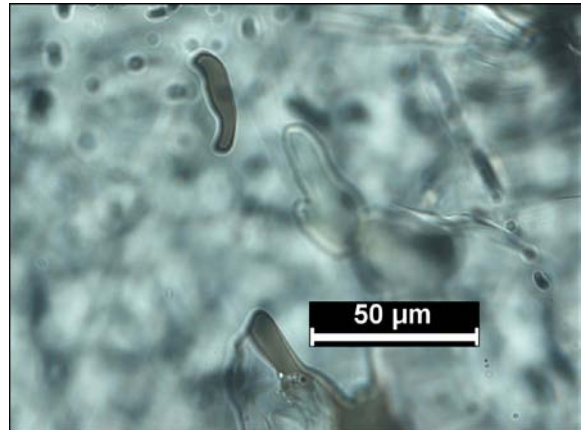
The white aggregates of fibrous celestine contain a relatively big number of fluid inclusions (Text-fig. 4). Most of the inclusions showed one phase – water solutions. Only a few inclusions contained two phases – liquid + vapor or two liquids of different proportions. There were also a wide range of sizes and shapes of fluid inclusions. The biggest size of a single inclusion did not exceed 50 mm. The finer inclusions (<10 mm) were mostly isometric, while coarser inclusions were elongated or irregular in shape. Very few inclusions contained organic fluid next to the water solution.

The pale-blue colored celestine contained many fewer fluid inclusions. Most of them represented water solutions. The maximum size of a single inclusion was up to 100 mm. Less than 5% of the observed inclusions contained vapor and liquid phases, the latter always dominating. Some inclusions showed a characteristic elongated shape (Text-fig. 5). A few inclusions contained hydrocarbons (Text-figs 6, 7).

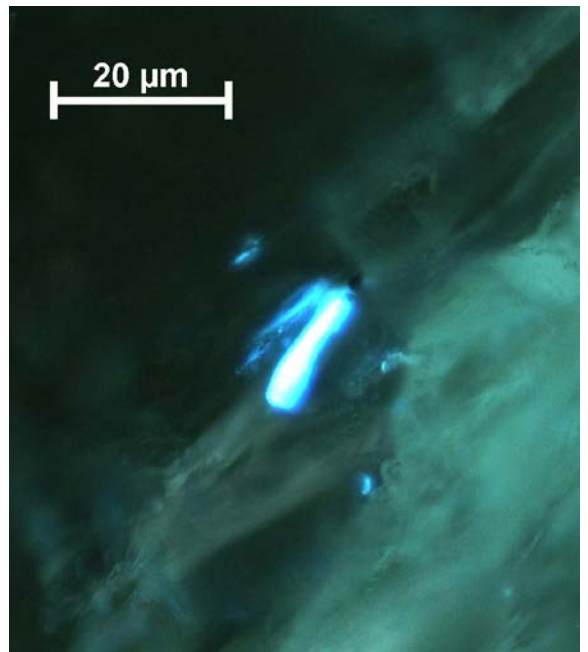
The brownish crystals of celestine also contained a relatively small number of fluid inclusions. A characteristic of inclusions containing water solutions was their irregular shape (Text-fig. 8). The maximum size of an inclusion did not exceed 150 mm. The typical



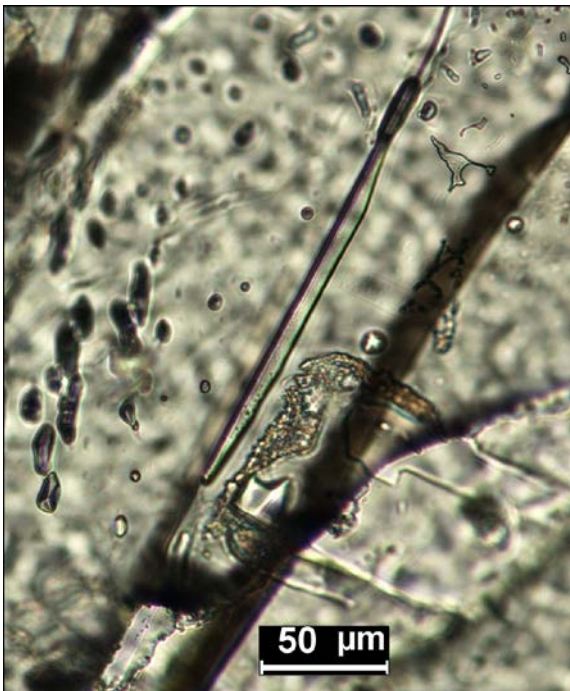
Text-fig. 4. Fluid inclusions in white fibrous celestine.



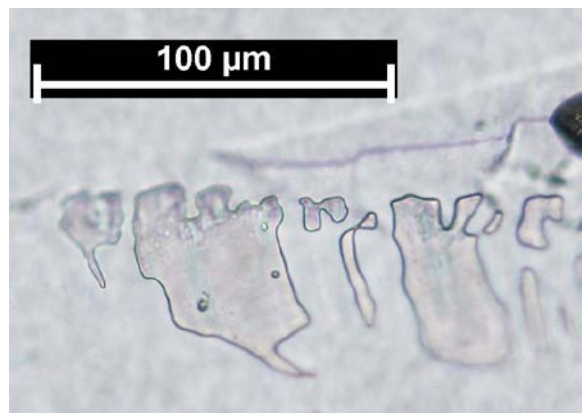
Text-fig. 6. Organic fluid inclusions in pale blue intergrowth celestine-strontianite



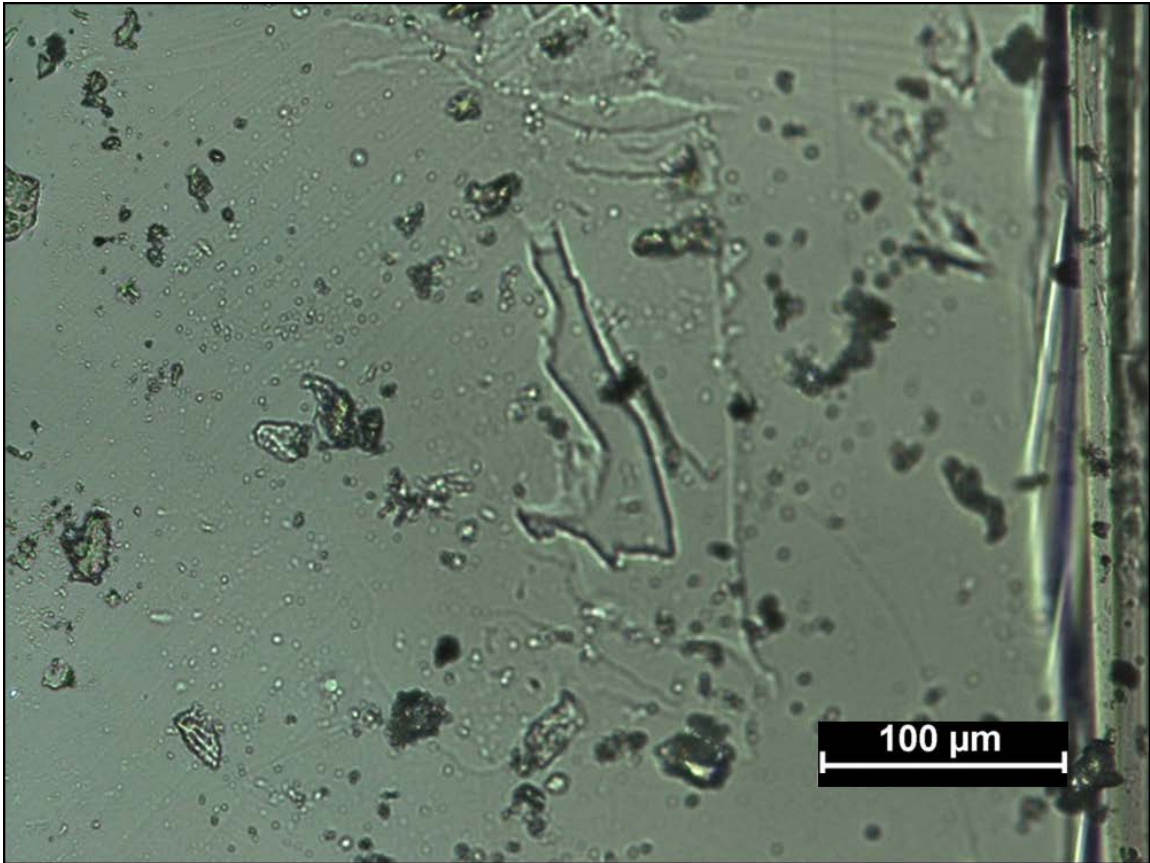
Text-fig. 7. Fluid inclusions in pale-blue celestine visible under UV.



Text-fig. 5. Fluid inclusions in pale blue intergrowth of celestine and strontianite.



Text-fig. 8. Fluid inclusions in brownish celestine.

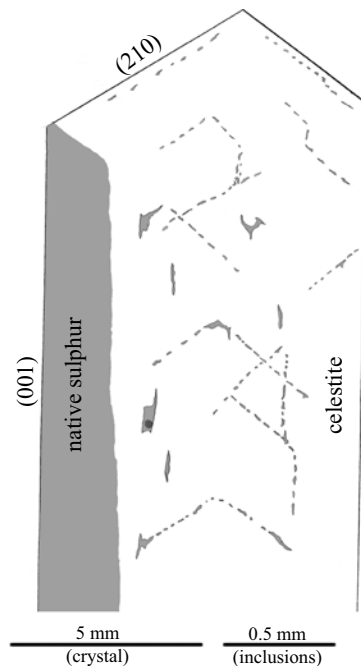


Text-fig. 9. Fluid inclusions in a single crystal of celestine.

size of inclusions fell in the range 5–25 mm. Some inclusions probably contained organic fluid. Their shape was elongated, their length achieving even 200 mm. Inclusions containing organic fluid + water fluid and water fluid + vapor phase were also observed.

The least amount of fluid inclusions was observed in prismatic single celestine crystals (Text-fig. 9). The maximum size of single fluid inclusion fell in the range 80–100 mm. Very few inclusions contained fluid other than water solution. It was observed that bigger inclusions, irregular in shape, were often connected by narrow channels.

Generally all four types of celestine examined contained a low number of fluid inclusions. The observed fluid inclusions are very similar in appearance, size and shape. Many of the inclusions, especially the smaller ones (<5 mm diameter), are arranged along trails parallel to the perfect (001) and good (210) cleavage of celestine (Text-fig. 10). This type of arrangement can represent a healed fracture or it can be an effect of recrystallization of originally bigger inclusions. These small inclusions were assumed to be of secondary origin or simply had too



Text-fig. 10. Arrangement of fluid inclusions in a big idiomorphic crystal of celestine.

		Salt conc. [wt % eq. NaCl]	NaCl [wt % of salt]	CaCl ₂ [wt % of salt]
MG-9	1	16	65	35
	2	18	69	31
	3	17	65	35
	4	15	80	20
	5	15	74	36
MG-22	1	16	64	36
	2	15	60	40
	3	18	68	32
	4	10	85	15
	5	17	60	40
	6	11	83	17
	7	14	81	19
	8	18	65	35
MG-2	1	17	66	34
	2	15	73	27
	3	14	70	30
	4	12	72	28
MG-12	1	14	69	31
	2	17	66	34
	3	15	65	35
	4	13	68	32
	5	15	69	31
	6	15	64	36
MG-13	1	14	71	29
	2	13	64	36
	3	15	73	27
	4	12	66	34
	5	12	68	32
	6	13	66	34
MG-14	1	14	59	41
	2	19	64	36
	3	20	67	33
	4	9	85	15
	5	12	71	29
	6	19	64	36
	7	10	88	12
	8	18	65	35
MG-1	1	7	80	20
	2	8	84	16
	3	9	82	18
	4	10	81	19
	5	8	80	20
MG-3	1	7	87	13
	2	6	90	10
	3	6	90	10
	4	8	91	9
	5	8	89	11
	6	7	89	11
	7	8	88	12

		Salt conc. [wt % eq. NaCl]	NaCl [wt % of salt]	CaCl ₂ [wt % of salt]
MG-5	1	12	90	10
	2	12	91	9
	3	9	90	10
	4	9	90	10
	5	10	88	12
	6	11	87	13
	7	9	89	11
	8	10	88	12
MG-6	1	15	68	32
	2	16	65	35
	3	17	69	31
	4	13	81	19
	5	10	90	10
	6	9	87	13
	7	12	77	23
	8	11	85	15
	9	13	83	17
MG-7	1	17	65	35
	2	15	69	31
	3	16	66	34
	4	14	80	20
	5	13	84	16
	6	11	85	15
	7	11	88	12
MG-8	1	15	68	32
	2	14	70	30
	3	10	87	13
	4	11	90	10

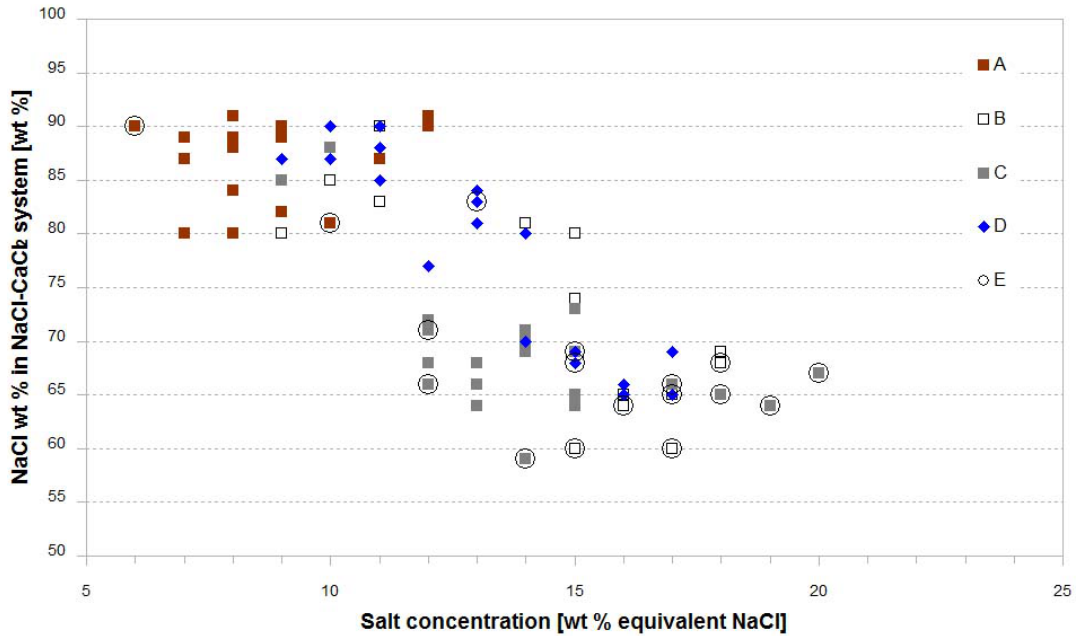
Table 1. Composition of fluid inclusions in celestine from Machów Mine.

small a size and were excluded from further investigation. Every type of sample examined revealed a few of the relatively big (>20 mm) fluid inclusions that were examined in this study.

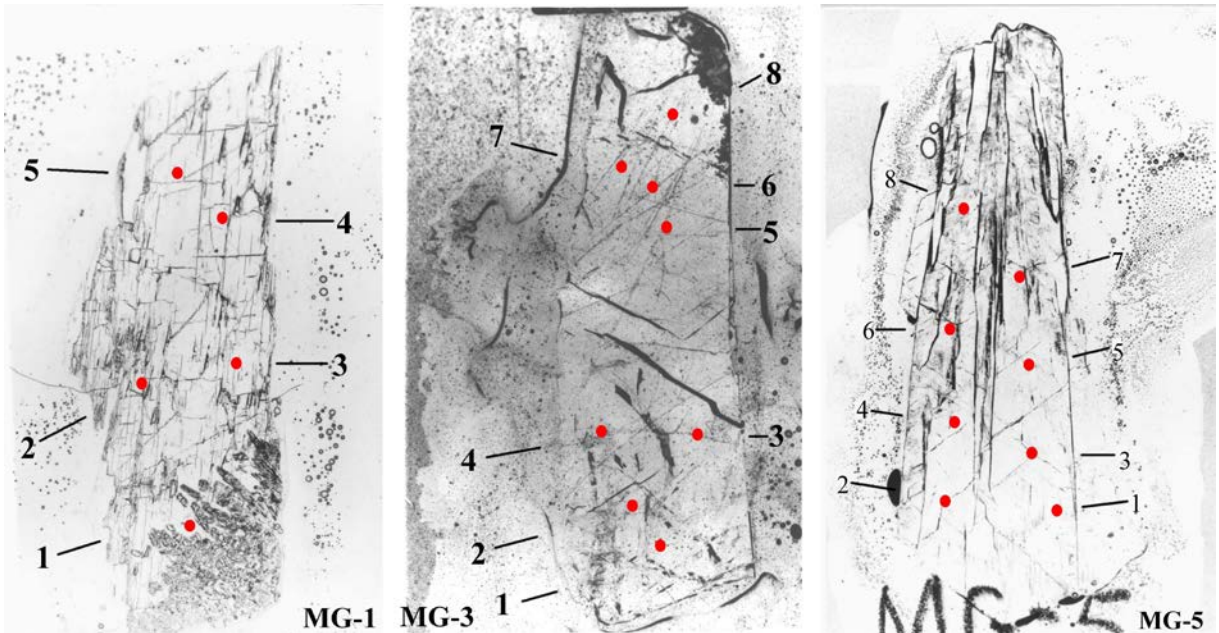
CHEMICAL COMPOSITION OF FLUID INCLUSIONS

Overall 80 fluid inclusions in celestine were successfully investigated using the method mentioned above. Additionally 20 of these inclusions contained some vapor phase which was separately analyzed. The data in Tables 1, 2 and Text-fig. 11 represent the results obtained.

From these data it is clear that it is possible to distinguish two main types of fluid inclusions in celestine.



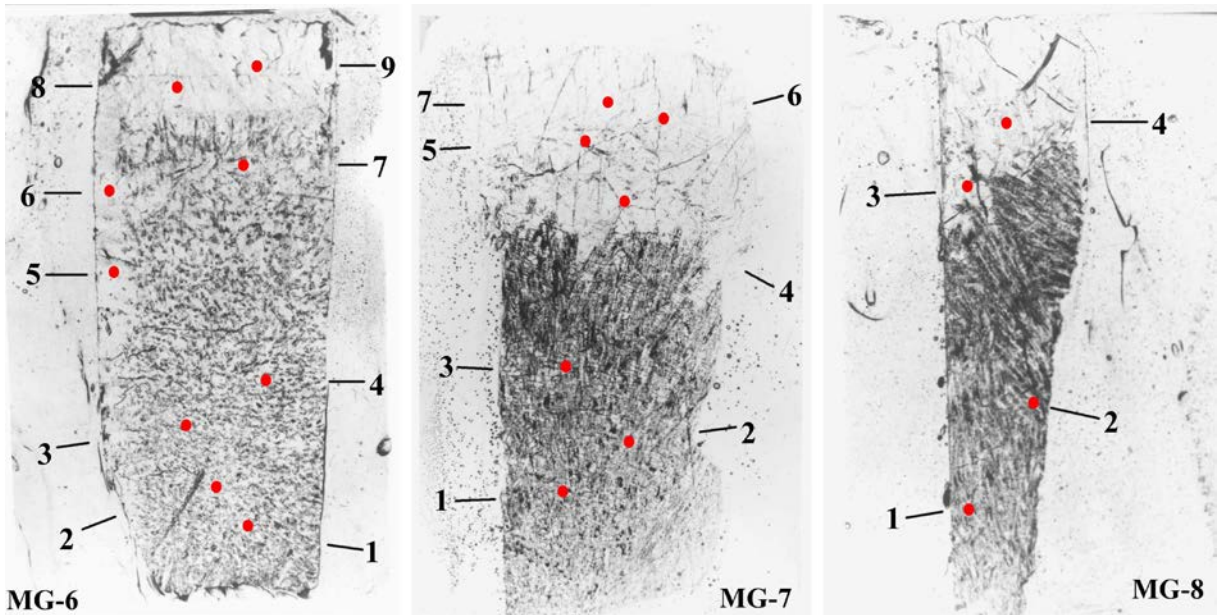
Text-fig. 11. Concentration of salt versus NaCl/CaCl₂ ratio for investigated fluid inclusion. A–D – fluid inclusions in different varieties of celestine (A – fan-shape brownish aggregates of acicular crystals, B – white, radial or parallel aggregates of fibrous celestine, C – single prismatic crystals or stellate aggregates, D – whitish wedge-shaped intergrowths with strontianite). Symbol E marks fluid inclusions containing methane.



Text-fig. 12. Distribution of fluid inclusions in the thin plates prepared from brownish celestine aggregates.

The first type is characterized by relatively high salinity (12–20 wt % NaCl), with elevated contents of CaCl₂ in the NaCl–CaCl₂ system (26–41 wt %). This type of inclusion often contains some gas phase – mainly methane. A similar composition was reported

for gases extracted from the borehole drilled before the opening the Machów mine. Methane was the dominant component (near 60 vol. %), while nitrogen (about 35%) and carbon dioxide (about 5%) were less abundant (Majka-Smuszkiewicz 1969).



Text-fig. 13. Distribution of fluid inclusions in the thin plates prepared from pale-blue celestine-strontianite aggregates (dark area represents strontianite).

The second type of fluid inclusion is characterized by relatively low salinity (6–12 wt % NaCl), and a high NaCl/CaCl₂ ratio (80–91 NaCl wt %). This type of fluid inclusion very rarely is connected with a vapor phase containing methane.

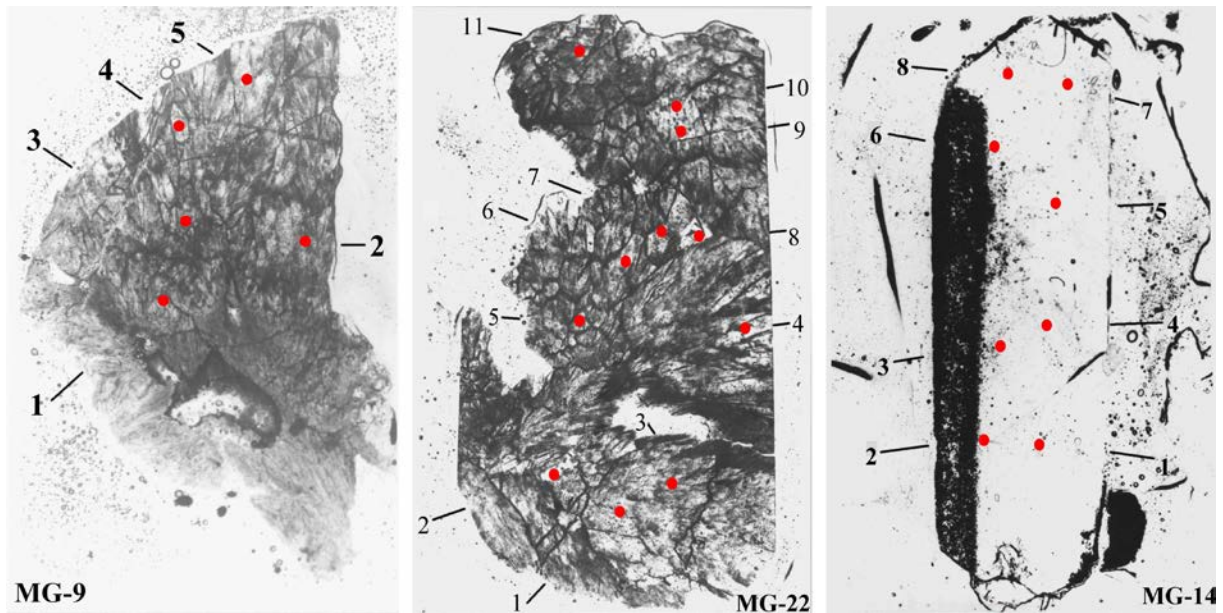
There is some correlation between the morphological type of celestine and the fluid inclusion type. Relatively large, well developed, clear crystals of celestine usually contain fluid inclusions of the second type, whereas brownish aggregates show the presence of the first type of inclusion only. The white fibrous celestine and celestine-strontianite intergrowths contain both types of inclusions as well as several inclusions of intermediate composition. It is worth noting that in both cases the salinity and NaCl/CaCl₂ ratio do not reach extreme values.

Further important information concerns the zonal ordering of the types of fluid inclusions in the investigated samples (Text-figs 12–15). In all mono-celestine samples no zoning occurs in the arrangement of fluid inclusions. But there is evident ordering of different types of fluid inclusions in samples containing celestine and strontianite aggregates (Text-fig. 13). The bottom parts of those aggregates containing strontianite include fluids of the first type, whereas the upper parts of the aggregates composed of celestine include fluids of the second type. A very similar zonation can be found in crystals containing native sulphur inclusions (Text-fig. 14, sample MG-

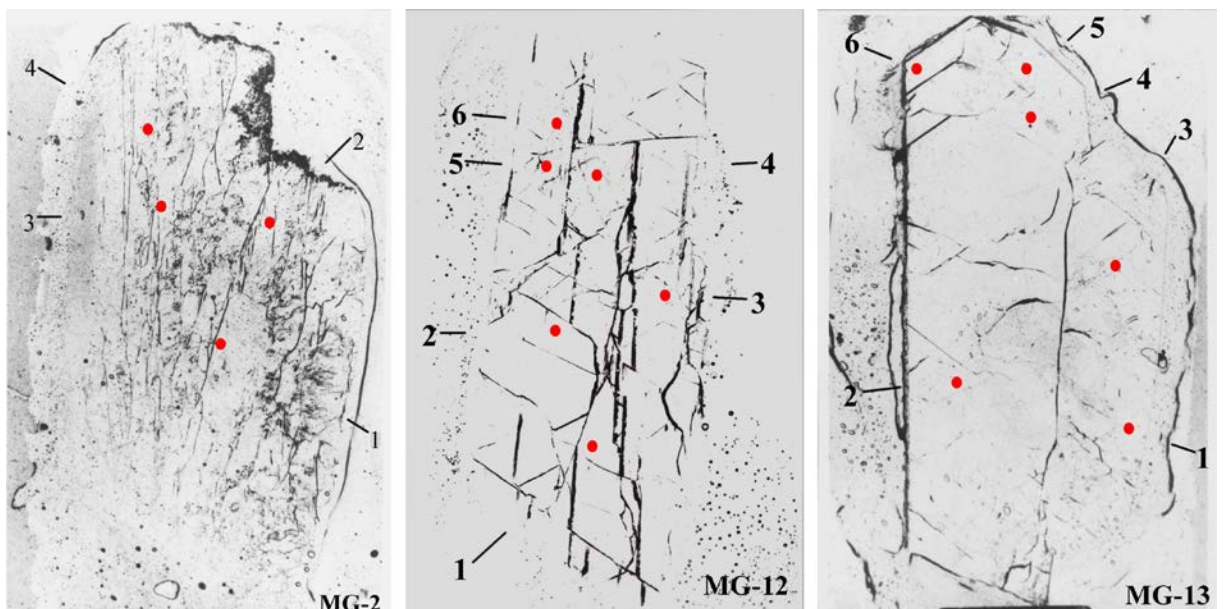
14). Zones of celestine closer to the native sulphur contain fluid inclusions of the first type, whereas zones in the outer parts of the crystal contain fluid inclusions of the second type.

		CH ₄ [Vol. %]	N ₂ [Vol. %]
MG-22	1	100	0
	2	100	0
	3	80	20
	5	100	0
	9	100	0
MG-2	1	82	18
MG-12	5	95	5
MG-13	4	84	16
MG-14	1	100	0
	2	89	11
	3	92	8
	5	86	14
	6	88	12
	8	84	16
MG-1	4	90	10
MG-3	2	91	9
MG-6	1	87	13
	9	100	0
MG-7	1	87	13

Table 2. Composition of gaseous phase in celestine's fluid inclusion from Machów Mine.



Text-fig. 14. Distribution of fluid inclusions in the thin plates prepared from white fibrous aggregates of celestine (MG-9 and MG-22) and from single crystals of celestine with inclusions of native sulphur (dark area) (MG-14).

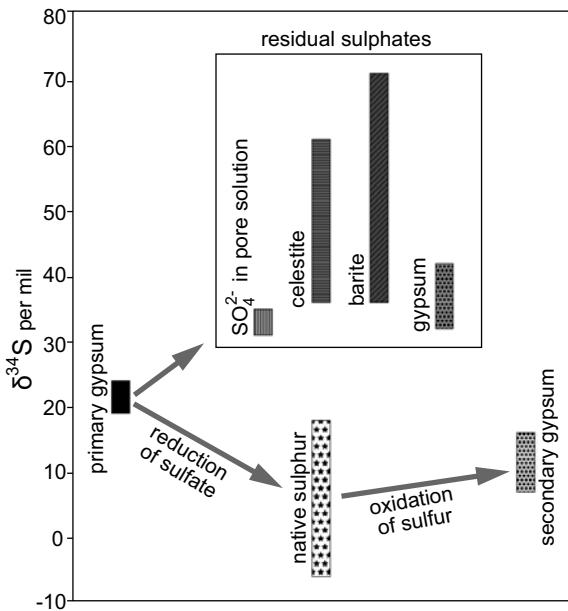


Text-fig. 15. Distribution of fluid inclusions in the thin plates prepared from single crystals of celestine.

DISCUSSION

This fluid inclusion study has allowed the recognition of two main stages of celestine crystallization. The first generation is characterized by higher salinity, higher $\text{CaCl}_2/\text{NaCl}$ ratio and often by the presence of methane, and we interpret this as connected with the final stages of the formation of native

sulphur deposits. The crystallization of the second, younger generation is the result of processes changing the chemistry of the original water by infiltration of meteoric water. This process is indicated by the lower salinity and lower $\text{CaCl}_2/\text{NaCl}$ ratio. The formation of the youngest generation of celestine could be connected with the beginning of mining activity – drainage and opening of the deposit. The composi-



Text-fig. 16. Sulphur isotope fractionation in the native sulphur deposits of Tarnobrzeg area (after Parafiniuk 1989).

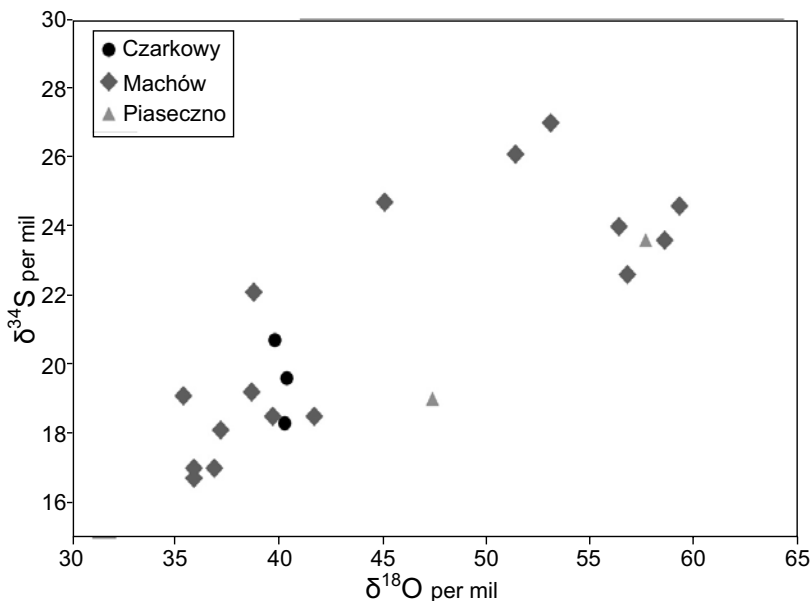
tion of the deposit waters before the start of exploitation reported by Majka-Smuszkiewicz (1969) shows Na⁺-Cl⁻ type (in gram-miliequivalents): 78–92% Cl⁻, 0–15% SO₄²⁺, 5% HCO₃⁻, 76–88% Na⁺, 5–15% Ca²⁺, 5% Mg²⁺. These results correspond well to the younger type of fluid inclusions in celestine.

We also observed two similar mineral generations

in the case of barite from Machów mine. The barite precipitated even inside the pipes of the mine drainage confirming its youngest formation.

The fluid inclusion data obtained are in good agreement with the results of the sulphur isotopic determinations of Parafiniuk and Hałas 1997). Celestine (and barite) from sulphur deposits are distinctly enriched in ³⁴S in comparison with primary evaporitic gypsum and native sulphur (Text-fig. 16). The heavy isotopic composition shows that the celestine crystallized from the solutions containing residual sulphates not consumed by sulphate-reduction bacteria. The sulphur isotope ratios in celestine (Text-fig. 17) also allows the distinction of two generations of this mineral. The older generation shows higher δ³⁴S values varying from 60 to 45 per mil whereas the younger one is less enriched in ³⁴S with δ³⁴S values of 42–35 per mil. These celestine generations can easily be correlated with those evaluated from fluid inclusion study. Interestingly, the residual sulphates are still preserved in the formation waters as indicated by the sulphur isotopic composition of its sulphate ion with δ³⁴S values ca. 35 per mil.

The oxygen isotope studies have allowed us to obtain the temperature of celestine crystallization. The maximum temperature was not higher than 47°C (Bottcher and Parafiniuk 1998). Most likely the formation temperature was even lower as indicated by the value of 39°C obtained from the CaCO₃-H₂O system (Parafiniuk *et al.* 1994). A similar temperature – 37°C – was reported by Pobierizski (1993) from thermobarogeochemical data. Our fluid inclusion study



Text-fig. 17. Sulphur and oxygen isotope composition in celestine from Carpathian Foredeep (after Parafiniuk and Hałas 1997).

has confirmed this observation. Most inclusions did not contain a vapor bubble, so the typical temperature of fluid inclusion trapping was near to the surface temperature.

CONCLUSIONS

The conditions of the crystallization of celestine, constrained by the fluid inclusions and stable isotope data, are essential for determining the genesis of the native sulphur deposits of the Carpathian Foredeep.

Celestine forms several morphological types including: compact aggregates of radial or parallel white fibrous crystals; prismatic, well developed, transparent crystals; clusters of brownish, acicular idiomorphic crystals and pale blue, stubby crystals with strontianite in the bottom parts.

The composition of the fluid inclusions allowed us to distinguish two genetic groups of celestine. The first group with higher salinity (12–20 wt. % NaCl), higher content of CaCl₂, often with a methane bubble, represents an older generation of celestine. The inclusions of the younger celestine generation have a lower salinity (6–12 wt. % NaCl), higher NaCl/CaCl₂ ratio and occasionally contain methane.

The composition of the inclusions can be correlated with the morphological types of celestine and their sulphur isotope composition. The older celestine generation with the $\delta^{34}\text{S}$ values of 60–45 per mil formed during the final stage of sulphate reduction processes whereas the younger celestine characterized by $\delta^{34}\text{S}$ of 42–35 per mil crystallized from depositional water modified by the influence of meteoric waters.

Acknowledgements

The authors would like to thank the paper's reviewers.

REFERENCES

- Bąbel, M. 2004. Badenian evaporate basin of the northern Carpathian Foredeep as a drawdown salina basin. *Acta Geologica Polonica*, **54**, 313–337.
- Botcher, M. and Parafiniuk, J. 1998. Methane-derived carbonates in a native sulfur deposit: stable isotope and trace element discrimination related to the transformation of aragonite to calcite. *Isotopes Environmental Health Studies*, **34**, 177–190.
- Gąsiewicz, A. 2000a. Sedimentology and diagenesis of gypsum-ghost limestones and origin of Polish native sulphur deposits. *Prace Instytutu Geologicznego*, **172**, 1–143. [In Polish]
- Gąsiewicz, A. 2000b. Comparative study of major element geochemistry of gypsum-ghost limestones and selenite lithofacies from the Miocene of northern Carpathian Foredeep: implication to the model of massive replacement of solid sulphates by calcium carbonates. *Chemical Geology*, **164**, 183–218.
- Goldstein, R.H. 2001. Fluid inclusions in sedimentary and diagenetic systems. *Lithos*, **55**, 159–193.
- Kasprzyk, A., Pueyo, J., Hałas, S. and Fuenlabrada, J. 2007. Sulphur, oxygen and strontium isotope compositions of Middle Miocene (Badenian) calcium sulphates from the Carpathian Foredeep, Poland: palaeoenvironmental implications. *Geological Quarterly*, **51**, 285–294.
- Klimchouk, A. 1997. The role of karst in the genesis of sulphur deposits, Pre-Carpathian region, Ukraine. *Environmental Geology*, **31**, 1–20.
- Kozłowski, A. 1984. Calcium-rich inclusion solutions in fluorite from the Strzegom pegmatites. Lower Silesia. *Acta Geologica Polonica*, **34**, 131–138.
- Kowalski, W., Osmólski, T. and Pilichowska, E. 1980. Strontianite from the sulphur deposit of the Machów mine (SE Poland). *Archiwum Mineralogiczne*, **36**, 29–50. [In Polish]
- Krouse, H.R. and McCready, R.G.L. 1979. Reductive reactions in the sulfur cycle. In: Trudinger, P.A. and Swaine, D.J. (Eds), Biogeochemical cycling of mineral-forming elements, 315–368. Elsevier, Amsterdam, New York.
- Majka-Smuszkiewicz, A. 1969. Chemical composition of Tertiary waters in the region of Machów. *Kwartalnik Geologiczny*, **13**, 629–642. [In Polish]
- Nieć, M. and Sermet, E. 2023. Discovery, geological investigation, mining and future of sulphur deposits in Poland. *Przegląd Geologiczny*, **71**, 631–638. [In Polish]
- Osmólski, T. 1976. Karst and genesis of Polish sulphur deposits. *Kwartalnik Geologiczny*, **17**, 310–325. [In Polish]
- Parafiniuk, J. 1989a. Strontium and barium minerals in the sulphur deposits from Tarnobrzeg region (SE Poland). *Archiwum Mineralogiczne*, **43** (2), 41–64. [In Polish]
- Parafiniuk, J. 1989b. Oxidation of native sulfur in the Fore-Carpathian sulfur deposits in the light of isotopic and mineralogical data. *Acta Geologica Polonica*, **39**, 113–122.
- Parafiniuk, J. 2023. Minerals of the Tarnobrzeg native sulphur deposit. *Przegląd Geologiczny*, **71**, 605–613. [In Polish]
- Parafiniuk, J. and Hałas, S. 1997. Sulfur- and oxygen-isotope composition as the genetic indicator for celestine from the Miocene evaporates of the Carpathian Foredeep. *Slovak Geological Magazine*, **3**, 131–134.
- Parafiniuk, J., Kowalski, W. and Hałas, S. 1994. Stable isotope geochemistry and the Genesis of the Polish native sulphur deposits – a review. *Geological Quarterly*, **38**, 473–496.
- Parnell, J., Honghan, C., Middleton, D., Haggan, T. and Carey,

- P. 2000. Significance of fibrous mineral veins in hydrocarbon migration: fluid inclusion studies. *Journal of Geochemical Exploration*, **69–70**, 623–627.
- Pawlikowski, M. 2023. Formation of the sulfur deposit. Tarnobrzskie zagłębienie siarkowe od odkrycia złóż siarki do cudu ekologii. Konferencja historyczno-ekologiczna, 29–34. Muzeum – Zamek Tarnowskich w Tarnobrzegu; Tarnobrzeg. [In Polish]
- Pawłowski, S., Pawłowska, K. and Kubica, B. 1985. Geology of the Tarnobrzeg native sulphur deposit. *Prace Instytutu Geologicznego*, **114**, 1–109. [In Polish]
- Peryt, T.M., Szaran, J., Jasionowski, M., Hałas, S., Peryt, D., Poberezhsky, A., Karoli, S. and Wójtowicz, A. 2002. S and O isotope composition of the Badenia (Middle Miocene) sulphates In the Carpathian Foredeep. *Geologica Carpathica*, **53**, 391–398.
- Pilichowska, E. 1984. Crystallography of celestine from the sulphur deposit at Machów, south-central Poland. *Archiwum Mineralogiczne*, **40**, 23–40. [In Polish]
- Pobierizski, A. 1993. Use of thermobarogeochemical methods for the fluid inclusion studies in minerals of the sulfur deposits of the Carpathian Foredeep, West Ukraine. *Przegląd Geologiczny*, **41**, 835–841.
- Roedder, E. 1984. Fluid inclusions: M.S.A. *Reviews in Mineralogy*, **12**, 1–644.
- Ślęczka, A. and Oszczytko, N. 2002. Paleogeography of the Badenian Salt Basin (Carpathian Foredeep, Poland and Ukraine). *Geologica Carpathica*, special issue, **53**, 17–19.
- Van den Kerkhof, A. and Hein, U. 2001. Fluid inclusions petrography. *Lithos*, **55**, 27–47.
- Williams-Jones, A. and Samson, I. 1990. Theoretical estimation of halite solubility in the system NaCl-CaCl₂-H₂O: Application to fluid inclusions. *Canadian Mineralogist*, **28**, 299–304.

Manuscript submitted: 13th January 2025

Revised version accepted: 6th March 2025